Laser Induced Synthesis of Nickel Alloy (Alumel) Nanoparticles in Liquids

C.G. Moura[1,*], C. Cano-Raya[2], J.P.F. Grilo[3], J.C. Viana[2], Z.Z. Denchev[2], R.M. Nascimento[4] and F.S. Silva[1]

[1]*CMEMS-UMinho, University of Minho, Campus de Azurém, 4800-058, Guimarães, Portugal*

[2]*IPC/i3N – Institute for Polymers and Composites, University of Minho, Campus de Azurém, 4800-058 Guimarães, Portugal*

[3]*Department of Materials and Ceramics Engineering, University of Aveiro, 3810-193, Aveiro, Portugal*

[4]*Federal University of Rio Grande do Norte, UFRN, 59078-970 Natal, Brazil*

Abstract: Pulsed laser ablation in liquids (PLAL) has been growing as a powerful technique for the synthesis of multielement nanoparticles (NPs) such as metal alloys with complex composition. In consequence, there is a great necessity in expanding the current knowledge about alloy NPs formation during this method, aiming to control the chemical composition of produced NPs. In this work, a nanosecond Nd:YAG laser was used to synthesize NPs of a novel nickel (Ni) alloy, and a brief description regarding the influence of liquid media in size and stability of produced nanoparticles is presented. The results showed great stability in the colloids produced in isopropanol medium without using a surfactant, whereas this environment allowed the production of smaller nanoparticles.

Keywords: Nickel alloy, laser ablation, nanoparticles, Nd:YAG laser, band gap.

1. INTRODUCTION

The focus on metal nanoparticle research has become increasingly intense owing to their unique properties compared with bulk material, which allow many potential applications, including biology, medicine, electronics, energy conversion, linear and non-linear optics [1-4]. Among these applications, several works have shown the importance of obtaining metal alloy nanoparticles (NPs) with a low melting point in comparison to bulk material, since it can be dramatically decreased when the size of the substances is reduced to nanometer size [5]. The interest in the melting of metal particles at lower temperatures is triggered by recent studies referring to different applications field [6-9]. As an example, we can mention studies concerning laser-induced melting of mono and bimetallic NPs, which are nanometers sized and might become liquid at low temperatures, even if their bulk metal temperature is hundreds of degrees higher [10-13].

Among the techniques for producing NPs, pulsed laser ablation in liquids (PLAL) has stood out in recent years for being a versatile and an environmentally friendly technique to produce stable colloidal solutions with absence of chemical reagents and harmful materials [2,14-16]. In this method, a target material immersed in a liquid medium is irradiated by an ultra-short laser pulse, which causes the removal of material from target and formation of nanoparticles through nucleation and growth [15].

Besides, for obtaining multicomponent or alloy NPs with unconventional composition, that are not accessible by traditional methods, PLAL is preferable due to its fast kinects of NP formation and its potential to form high purity products [17].

The interest in synthesis of alloy NPs have increased, since these materials have altered properties relative to mono-metal nanoparticles. Among them, metal Ni alloys are of having huge attention in technology, because of their superior physical and mechanical properties [18-22], that enable their use in various applications, such as photocatalytic performance [23], energy storage [24,25] and biomedical field [26]. Liu *et al*. [27] studied the morphological characteristics of Ni NPs produced by pulsed laser ablation in gas medium. They reported that varying the background gases, Ni-NiO core-shell were obtain. In Dudoitis *et al*. [28] Ni NPs were generated in air, using a Nd:YAG laser, in pulse regimes of 15 ns and 10 ps, describing the influence of laser intensity on the lattice temperature. Furthermore, Ni NPs production by PLAL was reported recently by Jaleh *et al*. [29] using a high repetition Nd:YAG laser for ablating pure Ni target in methanol with PolyVinylPyrrolodone (PVP) as stabilizer.

*Address correspondence to this author at the CMEMS-UMinho, University of Minho, Campus de Azurém, 4800-058, Guimarães, Portugal;
E-mail: caroline.materiais@gmail.com

Due to the enhancement of Ni alloys properties compared to pure metals, these materials also became promising to substitute noble metals in several applications. Recently, Marzun *et al*. [30] studied the properties of nickel-molybdenum system as catalysts in different sectors, to overcome platinum and iridium (which are rare and expensive metals), since Ni based materials show comparable catalytic performance with them. They have produced Ni-Mo alloy NPs using laser ablation in water and acetone and verified a significant increase in electrochemical activity, which means that these materials are attractive catalysts to replace noble metals.

Despite the previous investigations in literature, works concerning nickel-aluminum or nickel-aluminum-manganese-silicon system are very scarce. Nickel aluminides are technologically very interesting because they have higher melting point than pure aluminum and are lighter than pure nickel. Furthermore, the intermetallic phases have lattice structures that reduce the mobility of dislocation and diffusivity. Thus, superior mechanical properties at higher temperatures and corrosion resistivity are achieved [31]. However, these applications require rigorous processing of the materials, in which laser ablation in liquid comes into play as a promising approach for this purpose.

In this work, we synthesized and characterized novel nanoparticles of nickel alloy by using nanosecond laser ablation of a commercial alloy target (Alumel, 95% Ni, 2% Al, 2% Mn and 1% of Si). To the best of our knowledge, NPs from this purpose material have never been done by this method before. Here, we studied the effect of liquid medium on produced nanoparticles regarding size and shape. Their properties were investigated by several methods such as UV-Vis and TEM.

2. EXPERIMENTAL

The synthesis of Nickel alloy nanoparticles was performed using a 1064 nm high power Nd:YAG (*neodymium-doped yttrium aluminium garnet*) laser (OEM Plus, Italy) with an output power of 6W (corresponding to a laser fluence of 4244.0 J/cm²), spot size of 3 mm, pulse width ~35 ns and operated at the repetition rate of 20 kHz. The target sample used to carry out these experiments was 3 mm thick solid disk of Alumel ($Ni_{95}Mn_2Al_2Si_1$ - nickel-manganese-aluminum-silicon), immersed in a vessel filled with three different liquid media, namely distilled water (DW), isopropanol and ethanol. During each ablation process, a magnetic stirring was applied in order to avoid re-ablation of freshly formed nanoparticles, which would induce the broadening of size distribution via photoinduced fragmentation, besides decreasing the ablation rate. in each experiment, the ablation time was the same and corresponds to 11 minutes. In the case of the ablation process in DW medium, sodium dodecyl sulfate – SDS ($C_{12}H_{25}SO_4Na$) was used as a surfactant. The aqueous suspension was prepared by adding pure SDS powder to DW, carefully shaking to obtain a molar concentration of 0.025 mol/L. After the required processing time, the ablation process was interrupted, the Alumel colloidal solutions were stored for further analysis and dissolution processing.

The experimental setup chosen to produce Alumel NPs in liquid media is shown in Figure **1**.

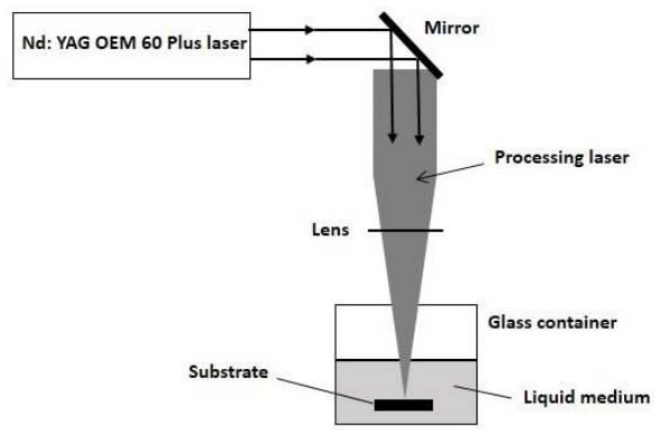

Figure 1: Schematic diagram of experimental setup for the fabrication of an Alumel colloidal suspension.

Alumel colloidal suspensions were characterized by optical absorbance spectroscopy and transmission electron microscope (TEM). Optical absorption spectra of the colloidal suspensions were recorded in the range from 190 to 800 nm of wavelength using an UV-Vis absorption spectrophotometer Model 2501 PC, Shimadzu. The pure solvent as used as reference to build the baseline. Observation of colloidal particles was performed by TEM (Hitachi 9000) at accelerating voltage of 300 kV. The samples were prepared by adding droplets of the colloidal solutions on carbon-coated copper grids. Two droplets of solution were deposited, and the grids dried in air. To evaluate the ablated nanoparticles composition, drops of each colloidal solution was deposited on silicon plate and dried in air. EDS analysis was performed on agglomerated particle of the Ni alloy, from a drop placed to air dry.

3. RESULTS AND DISCUSSION

3.1. Morphologies and Size Distribution of Metal Nanoparticles

As already known, composition of nanoparticles prepared by PLAL strongly depends on the liquid medium. Figure **2** shows the TEM images and analyzed data of Alumel nanoparticles produced by PLAL technique in three different ambient liquids: (a) DW+SDS solution, (b) ethanol and (c) isopropanol. The produced NPs are spherical with dimensions lower than 10 nm. The interaction of laser beam with Alumel in ethanol and isopropanol resulted in the production of extremely small particles (below 5 nanometers on average) in comparison to those produced in water medium. More details can be found in histograms presented in Figure **2**.

In the first condition, an aqueous solution of SDS (concentration 25 mM) was used as liquid medium to ablate Alumel target. SDS is used as a capping agent to prevent oxidation and the growth of the Alumel nanoparticles generated by laser ablation, encapsulating the newly formed NPs. Another important function of SDS is to act as a surfactant preventing NPs agglomeration. This is achieved by double layer that are formed around the nanoparticles by SDS molecule, in which the first layer has an orientation of hydrophilic part inward and hydrophobic part outward and the second layer has an opposite orientation [32,33].

Through TEM image (Figure **2a**), it is possible to observe that there was no aggregation, and this behavior can be attributed to the presence of SDS as surfactant, which plays a significant role in stability of the NPs. This process occurs due to electrostatic repulsion and hydrophobic interaction among the stabilizer's chains. Besides, NPs stability through ionic stabilizers is generally explained in terms of surfactant bilayer formation on the nanoparticles, which allows the alkyl groups to be held together by a hydrophobic bond, inhibit clusters aggregation, promoting NPs stabilization [34-36].

Generally, all liquid media allowed the formation of small nanoparticles with a narrow size distribution. In water medium, the particles size is between 2 and 10 nm, while in ethanol and isopropanol, the particles did not exceed 5 nm in a narrower distribution, being a men size of 2 and 1.8 nm, respectivelly. The mechanism of nanoparticles formation by laser ablation is not completely understood, mainly in production of metal alloys NPs field. Several ablation processes can occur simultaneously and may lead to deviations in the composition of the produced nanoparticles, where the energy density deposited on the target is quite important to the nanoparticle formation [17,37,38]. Due to the high laser fluence value applied here, we suppose that multiple ablation mechanisms, such as fragmentation, vaporization and phase explosion, were responsible for nanoparticle formation, leading to a narrow size distribution [17].

It is important to mention that the formation of NiO should not be ruled out, mainly in the case where Ni target was ablated in water, since oxidation–reduction processes may occur in this solvent. In this sense, the possibility of generating core-shell NPs of the type Ni-NiO and NiO-Ni should be considered [27,39,40]. Arbodela *et al*. [40] showed the formation of Ni and hollow Ni NPs when Ni target was ablated in *n*-heptane solution. Instead, for water, they found the formation of Ni oxide in different core-shell configurations. According to them, in water, the optical breakdown induced by laser ablation produces H_2 gas as byproduct from the reaction bellow

$Ni + H_2O \rightarrow NiO + H_2$ (1)

Besides, since during ns laser ablation high temperatures and pressures are easily reached in the plasma plume and in the plasma liquid-interface during a time interval compatible with the fast oxidation kinetics, it is possible that, under our experimental conditions, the previous reaction can easily generate oxidized species in the colloidal suspension [40,41].

In order to evaluate the composition of the ablated Alumel nanoparticles, a chemical analysis was performed for each condition. In this case, drops of the solution were placed on a silicon plate where it air-dried and then, the plate surface, containing agglomerated particles, was analyzed by EDS. The results are shown in Figure **3**. According to EDS analysis into the particle, all the alloy elements have been detected, being Ni in greater amount, as expected. In the case of water and SDS medium, because of the surfactant presence, the elements Na and S were also detected. The amount of oxygen can suggest the Ni alloy oxidation in ethanol and water liquid environment, which can be attributed to different aspects, such as the oxidation due to the interaction of particles deposited on the plate with the ambient air, and/or to the interaction of the particles with the liquid media during the ablation process.

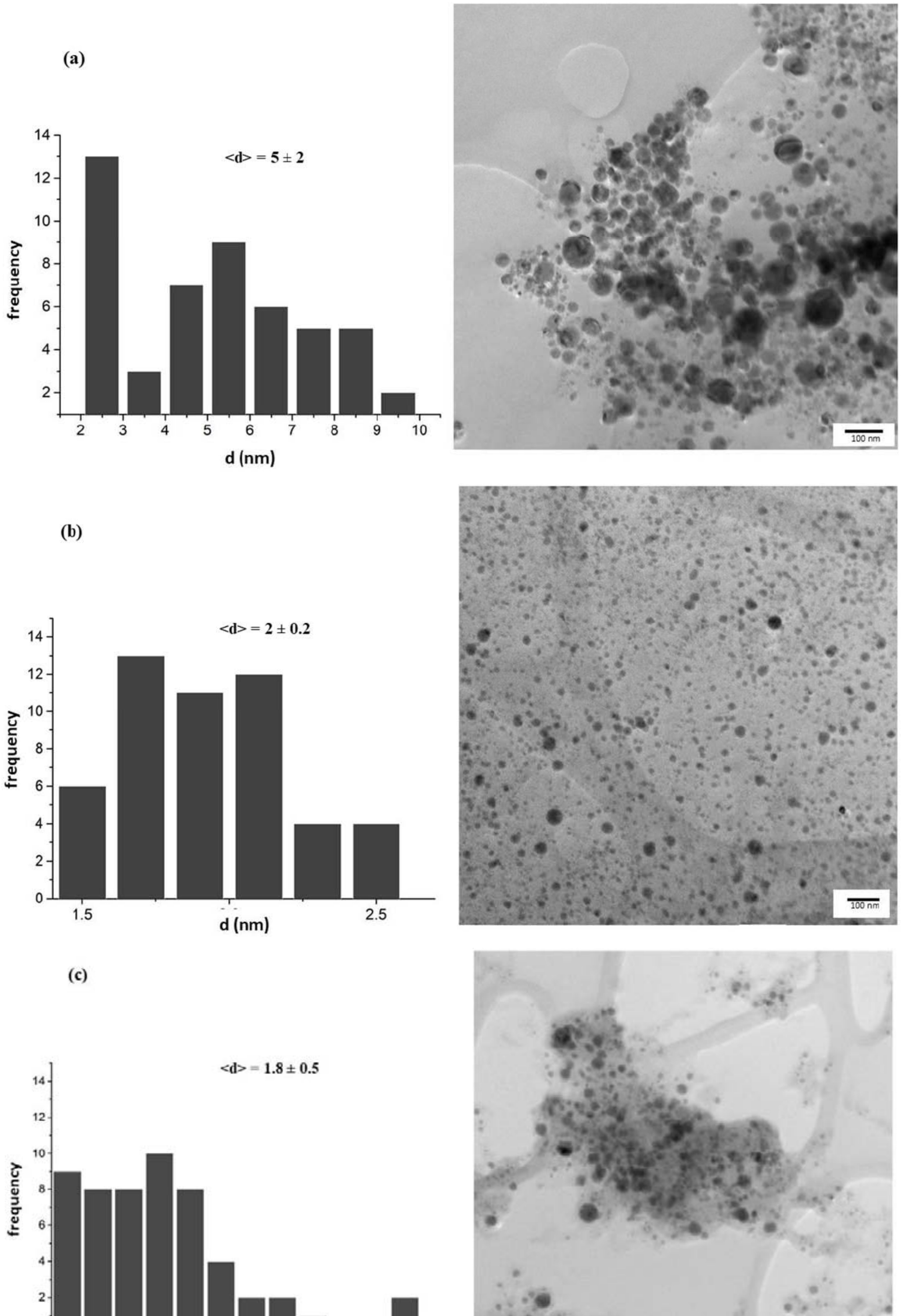

Figure 2: TEM images and calculated size and size distribution of Alumel nanoparticles produced in (**a**) distilled water + SDS, (**b**) ethanol and (**c**) isopropanol.

During PLAL, the ablated species interact with the solution and oxidized phases of the bulk material can be formed. The great amount of silicon is resulting from the silicon plate where the particles are deposited and also from the alloy composition. Thus, the EDS results show that nanoparticles of the alloy were formed, being composed by all the elements.

a)

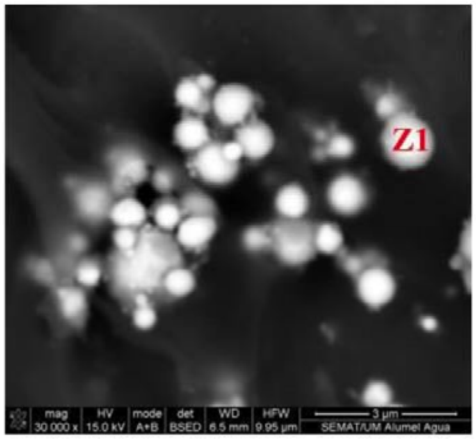

EDS **Z1**		
Element	Wt (%)	At (%)
O	7.07	18.96
Ni	77.12	56.32
Al	0.59	0.94
Mn	0.46	0.36
Si	9.64	14.72
Na	3.53	6.59
S	1.58	2.11

b)

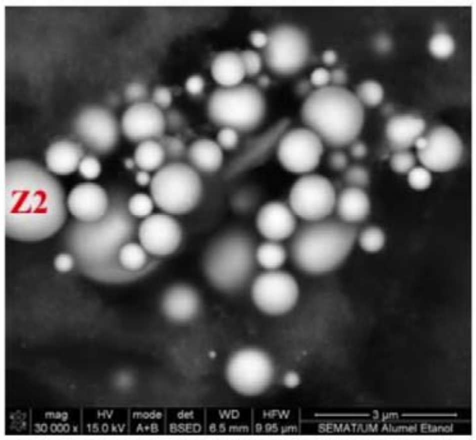

EDS **Z2**		
Element	Wt (%)	At (%)
O	4.30	13.34
Ni	88.16	74.49
Al	1.80	3.31
Mn	0.46	0.36
Si	4.27	7.53

Figure 3: STEM and EDS analysis of agglomerated particles from colloidal solution deposited on silicon plate. **a**) particles from water and SDS solution; **b**) particles from ethanol solution.

3.2. Optical Spectroscopy Analysis on the Interaction of Laser-Generated Nanoparticles and Liquid Medium

Colloidal solution of Alumel NPs ablated in different liquid media was measured by UV-Vis spectroscopy, monitoring spectra evolution in time. As can be seen in Figure **4a**, initially, colloidal solution of Alumel NPs produced in water medium, presents a characteristic surface plasmon resonance (SPR) absorption peak at 190 nm, declining smoothly toward longer wavelengths. This peak is probably due to the presence of colloidal Nickel as main metal component in the ablated nanoparticles [42]. After 24 days, this main peak is red shifted with 4 nm, shifting until a value of 7 nm after 1 month and 4 days. This bathochromic shift can be justified by the formation of a surrounding layer of metal oxides in the ablated nanoparticles [43]. After this period of time, a new absorption peak centered at 220 nm appears, possibly due to the presence of fully oxidized Alumel NPs [43].

Ethanol is also an infrared transparent liquid suitable for laser ablation. In this case, two SPR absorption peaks appear centered at 207 nm and 255 nm, respectively (Figure **4b**). The former peak is probably due to the existence of Alumel core-metal oxides shell structure and the latter should correspond to fully oxidized Alumel NPs. Characteristic peak of colloidal Nickel is not found this time, possibly due to the lack of a capping agent in solution. As regards the peaks evolution as a function of time, the intensity of the absorption peak centered at 207 nm decreases faster than the intensity of absorption peak centered at 255 nm. This fact could be explained by a higher tendency of partially oxidized NPs to undergo coalescence and settlement. Furthermore, the height of peaks decreased over the time. This spectral change can indicate that the diameters of the nanoparticles increase by aging effect, which means that metal NPs are aggregated and fused by, and hence the dispersity of NPs decreases over time [44]. The reduction in absorption intensity was more pronounced in ethanol in comparison to the other solvents.

In isopropanol (Figure **4c**), the stability of colloidal solutions over time was higher. Apart from being an

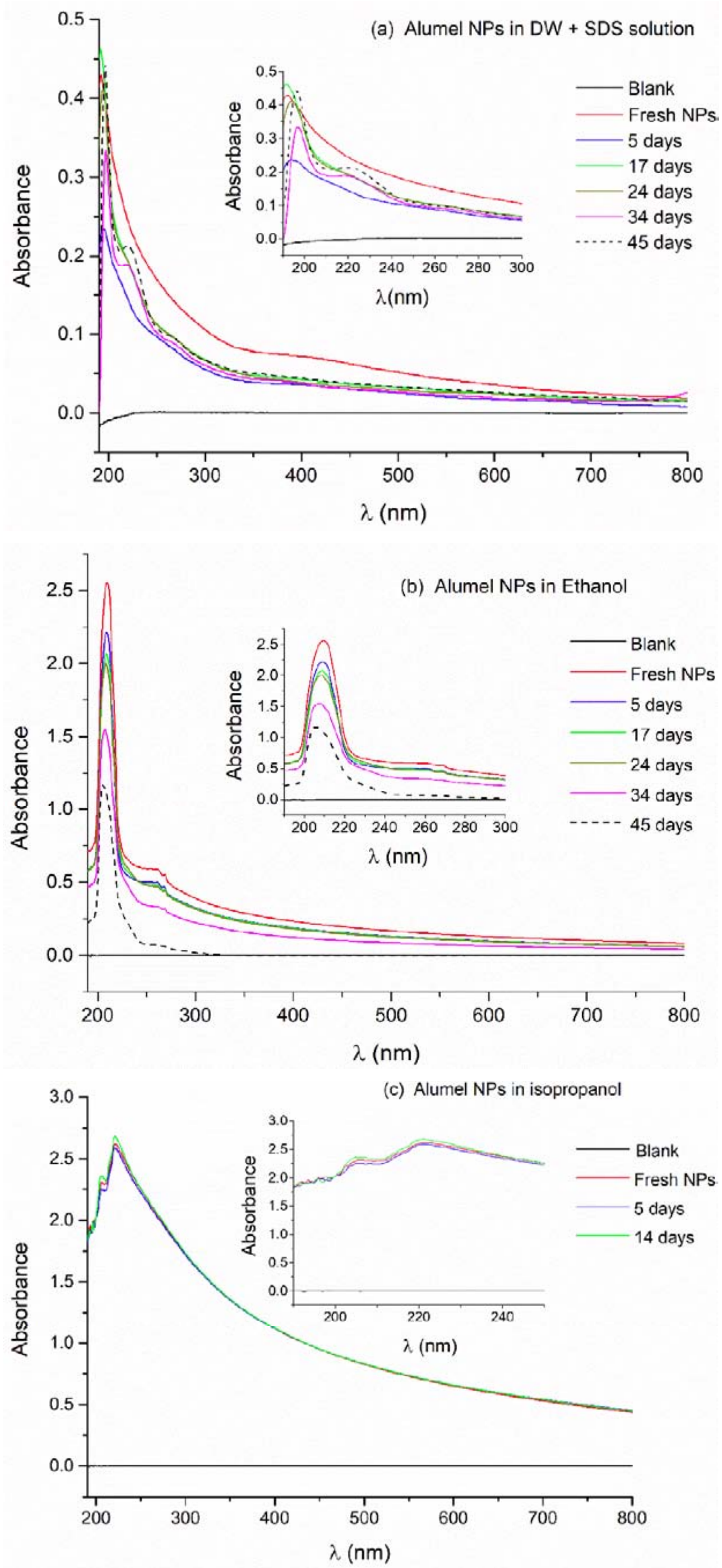

Figure 4: UV-Vis absorption spectra of (**a**) distilled water and SDS NPs colloidal solution, (**b**) ethanol and (**c**) isopropanol NPs colloidal solutions, measuring its evolution in time.

infrared transparent liquid, isopropanol proved to be an outstanding solvent to produce stable NPs colloidal solutions without the use of any protective agent. In ethanol environment, the characteristic peak of Nickel (at 190 nm) was not found because a capping agent was not used either. As can be seen, the mainly absorption peaks are centered around 220 nm. Regarding peaks evolution, no changes were observed for 14 days, which means that ablated Alumel NPs colloidal solutions were quite stable in these conditions. This stability of isopropanol as liquid medium has already been reported in the literature [45].

In general, under the studied conditions, all colloidal solutions showed certain stability over time, the isopropanol being the most stable liquid medium, although no surfactant was used in this case. However, a deeper study regarding composition and oxidation of the formed nanoparticles are crucial, mainly in the synthesis of NPs from multielement target. The presence of Ni alloy oxidation in the scope of the UV-vis spectroscopy can also be verified through the analysis of the band gap parameter. This oxidation presence of in the scope of the UV-vis spectroscopy can also be verified through the analysis of the band gap parameter. The band gap can be defined as the distance between the valence band (VB) of electrons and the conduction band (CB), and represents the minimum energy that is required to excite an electron up to a state in the conduction band so that it becomes free [46]. The optical band gap (Eg) can be obtained via the Tauc method [47], which is modulated as the tangent of the curve and extrapolated to the point where αhv(1/n) is zero. This method relates optical absorption strength with the photon energy, where h is the Planck's constant, v is the frequency of light, α is the absorption coefficient and the exponent n is related to the electronic of the band gap. In Figure **5** the band gap of the three fresh colloidal solutions produced in isopropanol, water and ethanol media were estimated to be 0.8 eV, 4.12 eV and 5.28 eV, respectively. These results clearly evidenced that through PLAL the band gap, and consequently, the electrical conductivity of the produced nanoparticles, depends on the surrounded liquid environment. The optical band gap of NiO particles has already been reported ranging from 3.4 eV to 4.3 eV [48]. Similarly, the band gap of Alumel NPs produced in water and ethanol fit into this range, typical of a semiconductor material. This result is aligned with the findings obtained through EDS analysis and confirms the formation of oxide specimens during the ablation process. On the other hand, the low band gap value related to the colloidal solution of NPs produced in isopropanol reflects the ability of this liquid medium to maintain the characteristics of the bulk material. In the light of foregoing, and despite the few studies regarding the addressed studied material for comparison purpose, the conducted analysis corroborates with previous findings and literature background [49–51], which allow to assert that the obtained outcome is reliable.

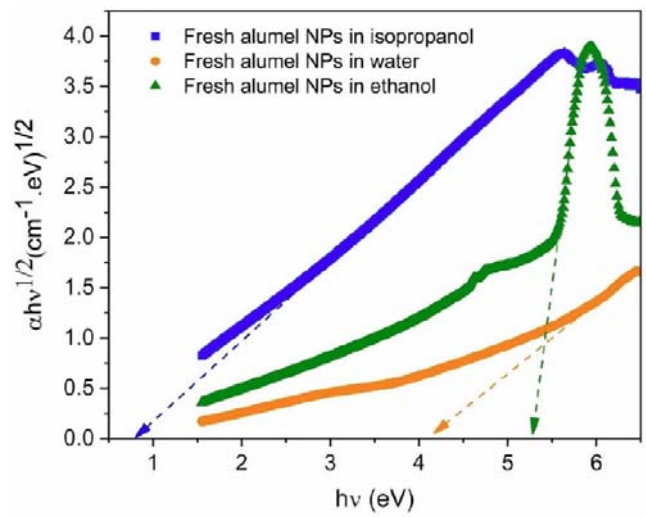

Figure 5: Optical band gap energy of the Alumel NPs produced in different liquid media.

4. CONCLUSIONS

Nickel alloy (Alumel) nanoparticles were successfully produced by pulsed laser ablation in water, ethanol and isopropanol environments. This method allows simple and fast production of Ni-based alloy NPs. The resulting colloidal solutions show the formation of stable Ni-NiO core-shell NPs. However, a precise analysis of stoichiometry composition of colloids is necessary, which is the next step for future works. In general, the produced NPs are spherical and present a small average particles size at tested conditions, which is attractive for many applications that require particles with a low melting point. In summary, the laser ablation in liquid medium is an alternative, efficient and free-contamination technique to produce stable nanoparticles solutions from a metal alloy target.

ACKNOWLEDGEMENT

This work has been supported by FCT (Fundação para a Ciência e Tecnologia – Portugal) in the scope of the projects UID/EEA/04436/2013 and NORTE-01-0145-FEDER-000018-HAMaBICo. It is also co-funded by National Funds through FCT - Portuguese Foundation for Science and Technology, Reference UID/CTM/50025/2013 and FEDER funds through the COMPETE 2020 Programme under the project number POCI-01-0145-FEDER-007688. Thank the CNPq (205791/2014-0) and CAPES for financial support.

REFERENCES

[1] H. Zeng, G. Duan, Y. Li, S. Yang, X. Xu, W. Cai, Blue luminescence of ZnO nanoparticles based on non-equilibrium processes: Defect origins and emission controls, Adv. Funct. Mater. 20 (2010) 561–572. https://doi.org/10.1002/adfm.200901884

[2] V. Amendola, D. Dini, S. Polizzi, J. Shen, K.M. Kadish, M.J.F. Calvete, M. Hanack, M. Meneghetti, Self-healing of gold nanoparticles in the presence of zinc phthalocyanines and their very efficient nonlinear absorption performances, J. Phys. Chem. C. 113 (2009) 8688–8695. https://doi.org/10.1021/jp810921w

[3] I. Papagiannouli, P. Aloukos, D. Rioux, M. Meunier, S. Couris, Effect of the composition on the nonlinear optical response of AuxAg1-x nano-alloys, J. Phys. Chem. C. 119 (2015) 6861–6872. https://doi.org/10.1021/jp512404a

[4] P. Golinska, M. Wypij, A.P. Ingle, I. Gupta, H. Dahm, M. Rai, Biogenic synthesis of metal nanoparticles from actinomycetes: biomedical applications and cytotoxicity, Appl. Microbiol. Biotechnol. 98 (2014) 8083–8097. https://doi.org/10.1007/s00253-014-5953-7

[5] H. Jiang, K. Moon, F. Hua, C.P. Wong, Synthesis and Thermal and Wetting Properties of Tin/Silver Alloy Nanoparticles for Low Melting Point Lead-Free Solders, Chem. Mater. 19 (2007) 4482–4485. https://doi.org/10.1021/cm0709976

[6] H. Friedman, S. Reich, R. Popovitz-Biro, P. Von Huth, I. Halevy, Y. Koltypin, A. Gedanken, Z. Porat, Micro- and nano-spheres of low melting point metals and alloys, formed by ultrasonic cavitation, Ultrason. Sonochem. 20 (2013) 432–444. https://doi.org/10.1016/j.ultsonch.2012.08.009

[7] H.R. Kotadia, P.D. Howes, S.H. Mannan, A review: On the development of low melting temperature Pb-free solders, Microelectron. Reliab. 54 (2014) 1253–1273. https://doi.org/10.1016/j.microrel.2014.02.025

[8] Y. Shu, K. Rajathurai, F. Gao, Q. Cui, Z. Gu, Synthesis and thermal properties of low melting temperature tin/indium (Sn/In) lead-free nanosolders and their melting behavior in a vapor flux, J. Alloys Compd. 626 (2015) 391–400. https://doi.org/10.1016/j.jallcom.2014.11.173

[9] F. Frongia, M. Pilloni, A. Scano, A. Ardu, C. Cannas, A. Musinu, G. Borzone, S. Delsante, R. Novakovic, G. Ennas, Synthesis and melting behaviour of Bi, Sn and Sn-Bi nanostructured alloy, J. Alloys Compd. 623 (2015) 7–14. https://doi.org/10.1016/j.jallcom.2014.08.122

[10] H. Fujiwara, S. Yanagida, P. V Kamat, Visible Laser Induced Fusion and Fragmentation of Thionicotinamide-Capped Gold Nanoparticles, J. Phys. Chem. B. 103 (1999) 2589–2591. https://doi.org/10.1021/jp984429c

[11] S. Link, C. Burda, B. Nikoobakht, M. a. El-Sayed, Laser-Induced Shape Changes of Colloidal Gold Nanorods Using Femtosecond and Nanosecond Laser Pulses, J. Phys. Chem. B. 104 (2000) 6152–6163. https://doi.org/10.1021/jp000679t

[12] H. Hodak, M. Giersig, H.I. Berlin, G. V Hartland, Laser-Induced Inter-Diffusion in AuAg Core - Shell Nanoparticles, (2000) 11708–11718. https://doi.org/10.1021/jp002438r

[13] T. Shibata, B.A. Bunker, Z. Zhang, D. Meisel, C.F. Vardeman, J.D. Gezelter, Size-dependent spontaneous alloying of Au-Ag nanoparticles, J. Am. Chem. Soc. 124 (2002) 11989–11996. https://doi.org/10.1021/ja026764r

[14] M.H. Mahdieh, B. Fattahi, Size properties of colloidal nanoparticles produced by nanosecond pulsed laser ablation and studying the effects of liquid medium and laser fluence, Appl. Surf. Sci. 329 (2015) 47–57. https://doi.org/10.1016/j.apsusc.2014.12.069

[15] V. Amendola, M. Meneghetti, What controls the composition and the structure of nanomaterials generated by laser ablation in liquid solution?, Phys. Chem. Chem. Phys. 15 (2013) 3027–3046. https://doi.org/10.1039/C2CP42895D

[16] H. Zeng, X.W. Du, S.C. Singh, S.A. Kulinich, S. Yang, J. He, W. Cai, Nanomaterials via laser ablation/irradiation in liquid: A review, Adv. Funct. Mater. 22 (2012) 1333–1353. https://doi.org/10.1002/adfm.201102295

[17] V. Amendola, M. Meneghetti, What controls the composition and the structure of nanomaterials generated by laser ablation in liquid solution?, Phys. Chem. Chem. Phys. 15 (2013) 3027–3046. https://doi.org/10.1039/c2cp42895d

[18] H. Bönnemann, R.M. Richards, Nanoscopic Metal Particles − Synthetic Methods and Potential Applications, Eur. J. Inorg. Chem. 2001 (2001) 2455–2480. https://doi.org/10.1002/1099-0682(200109)2001:10<2455::AID-EJIC2455>3.0.CO;2-Z

[19] J. Park, E. Kang, S.U. Son, H.M. Park, M.K. Lee, J. Kim, K.W. Kim, H.J. Noh, J.H. Park, C.J. Bae, J.G. Park, T. Hyeon, Monodisperse nanoparticles of Ni and NiO: Synthesis, characterization, self-assembled superlattices, and catalytic applications in the suzuki coupling reaction, Adv. Mater. 17 (2005) 429–434. https://doi.org/10.1002/adma.200400611

[20] L. Bai, F. Yuan, Q. Tang, Synthesis of nickel nanoparticles with uniform size via a modified hydrazine reduction route, Mater. Lett. 62 (2008) 2267–2270. https://doi.org/10.1016/j.matlet.2007.11.061

[21] G.G. Couto, J.J. Klein, W.H. Schreiner, D.H. Mosca, A.J.A. de Oliveira, A.J.G. Zarbin, Nickel nanoparticles obtained by a modified polyol process: Synthesis, characterization, and magnetic properties, J. Colloid Interface Sci. 311 (2007) 461–468. https://doi.org/10.1016/j.jcis.2007.03.045

[22] G. Murugadoss, M. Rajesh Kumar, Synthesis and optical properties of monodispersed Ni2+-doped ZnS nanoparticles, Appl. Nanosci. 4 (2014) 67–75. https://doi.org/10.1007/s13204-012-0167-8

[23] P. Pascariu, I.V. Tudose, M. Suchea, E. Koudoumas, N. Fifere, A. Airinei, Preparation and characterization of Ni, Co doped ZnO nanoparticles for photocatalytic applications, Appl. Surf. Sci. 448 (2018) 481–488. https://doi.org/10.1016/j.apsusc.2018.04.124

[24] S. Li, C. Shu, Y. Chen, L. Wang, A new application of nickel-boron amorphous alloy nanoparticles: anode-catalyzed direct borohydride fuel cell, Ionics (Kiel). 24 (2018) 201–209. https://doi.org/10.1007/s11581-017-2180-0

[25] K. Seevakan, A. Manikandan, P. Devendran, A. Shameem, T. Alagesan, Microwave combustion synthesis, magneto-optical and electrochemical properties of NiMoO4 nanoparticles for supercapacitor application, Ceram. Int. 44 (2018) 13879–13887. https://doi.org/10.1016/j.ceramint.2018.04.235

[26] W.T. Jhou, C. Wang, S. Ii, H. Sen Chiang, C.H. Hsueh, TiNiCuAg shape memory alloy films for biomedical applications, J. Alloys Compd. 738 (2018) 336–344. https://doi.org/10.1016/j.jallcom.2017.12.194

[27] B. Liu, Z. Hu, Y. Che, Y. Chen, X. Pan, Nanoparticle generation in ultrafast pulsed laser ablation of nickel, Appl. Phys. Lett. 90 (2007) 108–111. https://doi.org/10.1063/1.2434168

[28] V. Dudoitis, V. Ulevičius, G. Račiukaitis, N. Špirkauskaitė, K. Plauškaitė, Generation of metal nanoparticles by laser ablation, Lith. J. Phys. 51 (2011) 248–259. https://doi.org/10.3952/lithjphys.51302

[29] B. Jaleh, M.J. Torkamany, R. Golbedaghi, M. Noroozi, S. Habibi, F. Samavat, V.H. Jaberian, L. Albeheshti, Preparation of nickel nanoparticles via laser ablation in liquid and simultaneously spectroscopy, Adv. Mater. Res. 403–408 (2012) 4440–4444. https://doi.org/10.4028/www.scientific.net/AMR.403-408.4440

[30] G. Marzun, A. Levish, V. Mackert, T. Kallio, S. Barcikowski, P. Wagener, Laser synthesis, structure and chemical properties of colloidal nickel-molybdenum nanoparticles for the substitution of noble metals in heterogeneous catalysis, J. Colloid Interface Sci. 489 (2017) 57–67. https://doi.org/10.1016/j.jcis.2016.09.014

[31] J. Roth, H.R. Trebin, A. Kiselev, D.M. Rapp, Laser ablation of Al–Ni alloys and multilayers, Appl. Phys. A Mater. Sci. Process. 122 (2016) 1–13. https://doi.org/10.1007/s00339-016-9754-y

[32] F. Mafuné, J. Kohno, Y. Takeda, T. Kondow, H. Sawabe, Structure and Stability of Silver Nanoparticles in Aqueous Solution Produced by Laser Ablation, J. Phys. Chem. B. 104 (2000) 8333–8337. https://doi.org/10.1021/jp001803b

[33] F. Mafune, J. Kohno, Y. Takeda, T. Kondow, H. Sawabe, Formation and size control of sliver nanoparticles by laser ablation in aqueous solution, J. Phys. Chem. B. 104 (2000) 9111–9117. https://doi.org/10.1021/jp001336y

[34] Y.H. Chen, C.S. Yeh, Laser ablation method: Use of surfactants to form the dispersed Ag nanoparticles, Colloids Surfaces A Physicochem. Eng. Asp. 197 (2002) 133–139. https://doi.org/10.1016/S0927-7757(01)00854-8

[35] J. Hedberg, M. Lundin, T. Lowe, E. Blomberg, S. Wold, I.O. Wallinder, Interactions between surfactants and silver nanoparticles of varying charge, J. Colloid Interface Sci. 369 (2012) 193–201. https://doi.org/10.1016/j.jcis.2011.12.004

[36] S.K. Ridhima Chadha, Rajeshwar Sharma, Nandita Maiti, Anand Ballal, Effect of SDS concentration on colloidal suspensions of Ag and Au nanoparticles, Spectrochim. Acta Part a Mol. Biomol. Spectrosc. 150 (2015) 664–670. https://doi.org/10.1016/j.saa.2012.12.003

[37] L.J. Lewis, D. Perez, Laser ablation with short and ultrashort laser pulses: Basic mechanisms from molecular-dynamics simulations, Appl. Surf. Sci. 255 (2009) 5101–5106. https://doi.org/10.1016/j.apsusc.2008.07.116

[38] H.J. Dang, Z.H. Han, Z.G. Dai, Q.Z. Qin, Characterization of laser ablated species from a La–Ca–Mn–O target by angle- and time-resolved mass spectrometry, Int. J. Mass Spectrom. 178 (1998) 205–212. https://doi.org/10.1016/S1387-3806(98)14094-0

[39] S.Z. Khan, Y. Yuan, A. Abdolvand, M. Schmidt, P. Crouse, L. Li, Z. Liu, M. Sharp, K.G. Watkins, Generation and characterization of NiO nanoparticles by continuous wave fiber laser ablation in liquid, J. Nanoparticle Res. 11 (2009) 1421–1427. https://doi.org/10.1007/s11051-008-9530-9

[40] D. Muñetón Arboleda, J.M.J. Santillán, L.J. Mendoza Herrera, M.B.F. Van Raap, P. Mendoza Zélis, D. Muraca, D.C. Schinca, L.B. Scaffardi, Synthesis of Ni Nanoparticles by Femtosecond Laser Ablation in Liquids: Structure and Sizing, J. Phys. Chem. C. 119 (2015) 13184–13193. https://doi.org/10.1021/acs.jpcc.5b03124

[41] A. Nath, A. Khare, Size induced structural modifications in copper oxide nanoparticles synthesized via laser ablation in liquids, J. Appl. Phys. 110 (2011). https://doi.org/10.1063/1.3626463

[42] B.G. Ershov, Aqueous solutions of colloidal nickel: Radiation-chemical preparation, absorption spectra, and properties, Russ. Chem. Bull. 49 (2000) 1715–1721. https://doi.org/10.1007/BF02496340

[43] R. Singh, R.K. Soni, Laser synthesis of aluminium nanoparticles in biocompatible polymer solutions, Appl. Phys. A Mater. Sci. Process. 116 (2014) 689–701. https://doi.org/10.1007/s00339-014-8487-z

[44] M.A. Gondal, T.A. Saleh, Q.A. Drmosh, Synthesis of nickel oxide nanoparticles using pulsed laser ablation in liquids and their optical characterization, Appl. Surf. Sci. 258 (2012) 6982–6986. https://doi.org/10.1016/j.apsusc.2012.03.147

[45] M.-S. Yeh, Y.-S. Yang, Y.-P. Lee, H.-F. Lee, Y.-H. Yeh, C.-S. Yeh, C. Yeh, Formation and Characteristics of Cu Colloids from CuO Powder by Laser Irradiation in 2-Propanol, J. Phys. Chem. B. 103 (1999) 6851–6857. https://doi.org/10.1021/jp984163+

[46] X. Kang, S. Liu, Z. Dai, Y. He, X. Song, Z. Tan, Titanium dioxide: From engineering to applications, 2019. https://doi.org/10.3390/catal9020191

[47] J. Tauc, Optical properties and electronic structure of amorphous Ge and Si, Mater. Res. Bull. 3 (1968) 37–46.

[48] M.D. Irwin, D.B. Buchholz, A.W. Hains, R.P.H. Chang, T.J. Marks, p-Type semiconducting nickel oxide as an efficiency-enhancing anode interfacial layer in polymer bulk-heterojunction solar cells, Proc. Natl. Acad. Sci. U. S. A. 105 (2008) 2783–2787. https://doi.org/10.1073/pnas.0711990105

[49] P. Mallick, R. Biswal, Fe Doping Induced Shrinking of Band Gap of NiO Nanoparticles, Nanosci. Nanotechnol. 6 (2016) 59–61. https://doi.org/10.5923/j.nn.20160604.01

[50] M.N. Siddique, A. Ahmed, T. Ali, P. Tripathi, Investigation of optical properties of nickel oxide nanostructures using photoluminescence and diffuse reflectance spectroscopy, AIP Conf. Proc. 1953 (2018) 2–5. https://doi.org/10.1063/1.5032362

[51] F. Mustafa, S. Aslam, A. Jamil, M.A. Ahmad, Synthesis and characterization of wide band gap nickel oxide (NiO) powder via a facile route, Optik (Stuttg). 140 (2017) 38–44. https://doi.org/10.1016/j.ijleo.2017.04.029

Received on 16-03-2020   Accepted on 27-05-2020   Published on 01-07-2020

DOI: https://doi.org/10.31437/2414-2115.2020.06.2